Research Article

INDONESIAN SCHOLAR SOCIETY

Indones. J. Chem. Stud.
2025, 4(1), 22–27
Available online at journal.solusiriset.com
e-ISSN: 2830-7658; p-ISSN: 2830-778X

Indonesian Journal of Chemical Studies

Synthesis and Characterization of Titanium Dioxide/Graphene Nanoplatelets Nanocomposites via Planetary Ball Milling for Military Radar Absorbing Materials

Gita Resty Amalia[1], Andri Hardiansyah[2], Anselmo Bima Rasendriya[1], Ismail Rahmadtulloh[3,4], Andi Setiono[5], Riri Murniati[1]*

[1]*Department of Physics, The Republic of Indonesia Defense University, Bogor 16810, Indonesia*

[2]*Research Center for Nanotechnology Systems, National Research and Innovation Agency (BRIN), Banten 15314, Indonesia*

[3]*Department of Mechanical Engineering, National Taiwan University of Science and Technology, Taipei City 106335, Taiwan*

[4]*Department of Materials Engineering, Ming Chi University of Technology, New Taipei City 24301, Taiwan*

[5]*Research Center for Photonics, National Research and Innovation Agency (BRIN). Banten 15314, Indonesia*

Received: 25 Mar 2025; Revised: 17 Apr 2025; Accepted: 23 Apr 2025;
Published online: 8 Jun 2025; Published regularly: 30 Jun 2025

Abstract— Stealth technology is widely used in the military field to avoid enemy detection. Consequently, there has been a significant surge in research related to radar-absorbing materials (RAMs). Titanium dioxide (TiO_2) and graphene nanoplatelets (GNPs) are promising materials for developing RAMs. Combining TiO_2 as a semiconductor with GNPs as a conductive material could increase the ability to absorb microwaves through a more effective energy dissipation mechanism. In our study, TiO_2 and GNPs were fabricated using the planetary ball milling method. The structure and morphology of the resulting nanocomposites were evaluated using Field Emission Scanning Electron Microscopy with Energy Dispersive Spectroscopy with Energy Dispersive Spectroscopy (FE-SEM EDS) and X-ray Diffraction (XRD). FE-SEM observations showed that TiO_2 nanoparticles were attached to the surface of layered GNPs. XRD analysis showed a decrease in the peak intensity of the TiO_2/GNP nanocomposites compared to pure TiO_2 due to the addition of carbon elements. The performance of RAMs was evaluated using a Vector Network Analyzer (VNA) in the X-band (8-12 GHz) range with a 3-mm thickness. The VNA analysis indicated that the TiO_2/GNP nanocomposites exhibited the optimal reflection loss (RL) of -30.72 dB at a frequency of 8.42 GHz, accompanied by a through power of 99.91%. Consequently, TiO_2/GNP nanocomposites demonstrated promising potential as a military RAM.

Keywords— *Graphene nanoplatelets; Nanocomposites; Planetary ball milling; Radar absorbing material; Titanium dioxide*

1. INTRODUCTION

The development of stealth technology is currently experiencing rapid advancement, particularly in the military sector. To address the needs for such technology, radar-absorbing materials (RAMs) have been developed to produce materials that are effective in absorbing radar waves. The function of the radar system entails the transmission of electromagnetic signals, followed by the reception of echoes reflected from the observed object [1]. This key objective of this field is to create RAM materials with optimal dielectric properties. The rationale behind this assertion is that materials exhibiting favourable dielectric properties can conduct electromagnetic waves and convert them into heat effectively [2].

Carbon-based materials have promising dielectric properties, making them attractive for use as RAM. One suitable carbon-based material for this application is graphene nanoplatelets (GNPs). GNPs are stacks of flat graphene sheets, similar to the wall structure of carbon nanotubes but in a planar form. They are also known as graphite nanoplatelets, consisting of more than 10 graphene layers [3]. The characteristics of GNPs that make them suitable as RAM are lightweight, have good mechanical properties, large specific surface area of

***Corresponding author**.
Email address: ririmurniati90@gmail.com
DOI: 10.55749/ijcs.v4i1.67

20–40 m^2/g, and have excellent thermal and electrical conductivity values of 80,000 S/m [4]. Kumar et al. have synthesized GNPs composited with epoxy-silane functionalized cardanol, resulting in excellent absorption of -18 dB [5]. Silva et al. have synthesized GNPs/epoxy composites producing excellent microwave absorption material, resulting in a reflection loss of -13.5 dB [6].

In addition to carbon-based materials, semiconductor materials such as oxide ceramics have promising dielectric properties. TiO_2 is a semiconductor with excellent dielectric properties, high-temperature resistance, low density, and non-toxic material, which improves the conductivity of the RAMs and is suitable for composite fabrication [7–9]. Previous studies have also shown that TiO_2 crystals are amorphous due to oxygen-containing functional groups that cause polarization loss, leading to optimal impedance matching and minimized attenuation caused by related relaxation and interfacial polarization [10, 11].

Combining carbon materials with semiconductors is an efficacious innovation in developing more optimized RAM. Zhang, et al. have synthesized TiO_2/rGO using the solvothermal method and obtained a reflection loss value of -42.8 dB at 8.72 GHz [10]. Mo, et al. have studied the synthesized of CNT/TiO_2, obtaining a reflection loss value of -31.8 dB at 10.35 GHz using the hydrolysis and heat treatment methods [12].

In this study, carbon-based and semiconductor materials are synthesized to generate TiO_2/GNP nanocomposites using the planetary ball milling method. This method offers a simple process and is a type of green synthesis because it does not use toxic compound solvents. The use of GNPs in RAM applications remains underutilized, thus classifying this research as a novel innovation. The structure and morphology are characterized using Field Emission Scanning Electron Microscopy with Energy Dispersive Spectroscopy (FE-SEM EDS) and X-ray Diffraction (XRD). The RAM performance is evaluated using a Vector Network Analyzer (VNA) in the X-band frequency range (8-12 GHz) to assess the effectiveness of the material in absorbing electromagnetic waves.

2. EXPERIMENTAL SECTION

2.1. Materials

Titanium(IV) oxide (TiO_2) M=79.87 g/mol and graphene nanoplatelets (GNPs) grade C-750 M=12.01 g/mol were purchased from Sigma Aldrich, USA.

2.2. Instrumentation

The nanocomposites were homogenized using the planetary ball milling from Retsch, Germany. The surface morphology and composition of nanocomposites were observed using Field Emission Scanning Electron Microscopy with Energy Dispersive Spectroscopy (FE-SEM EDS) JEOL JSM-IT700HR, Japan. The lattice characteristics of the nanocomposites were measured using an X-Ray diffractometer (XRD) PANalytical X'pert, Netherlands. The microwave absorption performance of the nanocomposites was evaluated using a Vector Network Analyzer (VNA) Anritsu MS2038C, Japan.

2.3. Synthesis of Nanocomposites

Nanocomposites were synthesized using commercial TiO_2 and GNPs homogenized using the planetary ball milling method. The homogenization process was carried out using stainless steel balls for 3 h at 300 rpm to ensure optimal mixing. The ratio of TiO_2 and GNPs used was 1:1. After the milling process, the samples were filtered using a 400-mesh sieve to obtain a uniform particle size and remove impurities in the material.

2.4. Structure and Morphology Characterization

FE-SEM characterization used an accelerating voltage of 10 kV in secondary electron mode with an image magnification of 50,000× for GNPs and 4,000× for TiO_2/GNP nanocomposites. XRD characterization used a voltage of 40 kV, a current of 30 mA, and incident angle of 1° with a 2θ range of 20°-90°.

2.5. Microwave Absorption Performance

VNA testing used a dual-port VNA that produced S_{11}, S_{12}, S_{21}, and S_{22} parameters in the X-band frequency range (8-12 GHz) with a material thickness of 3mm.

3. RESULT AND DISCUSSION

3.1. Formation Mechanism

The formation of TiO_2/GNPs nanocomposites using planetary ball milling resulted in smaller particle sizes. This condition is due to the continuous impact of the milling balls, which causes a reduction in the size of TiO_2 and increases its surface area. In the case of GNPs, the constant impact results in the production of smaller and thinner graphene sheets. The ball milling process also causes physical bonding between TiO_2 and GNPs, called the mechanical interlocking model caused by the collision between the two materials. This model is determined by mechanical interlocking and adhesive bonds [13, 14]. The mixing these two materials lead to a homogeneous mixture of TiO_2 and GNPs, forming the TiO_2/GNPs nanocomposites. Schematic representation of formation mechanism of TiO_2/GNPs nanocomposites can be seen in **Fig. 1.**

3.2. Structure and Morphology Analysis

Fig. 2A shows the FE-SEM image GNPs. GNPs exhibited a layered surface structure. This layered

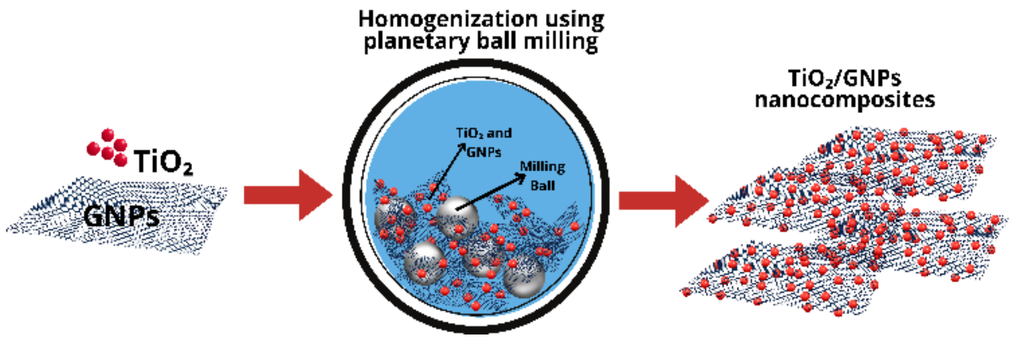

Fig. 1. Schematic representation of formation mechanism of TiO_2/GNPs nanocomposites

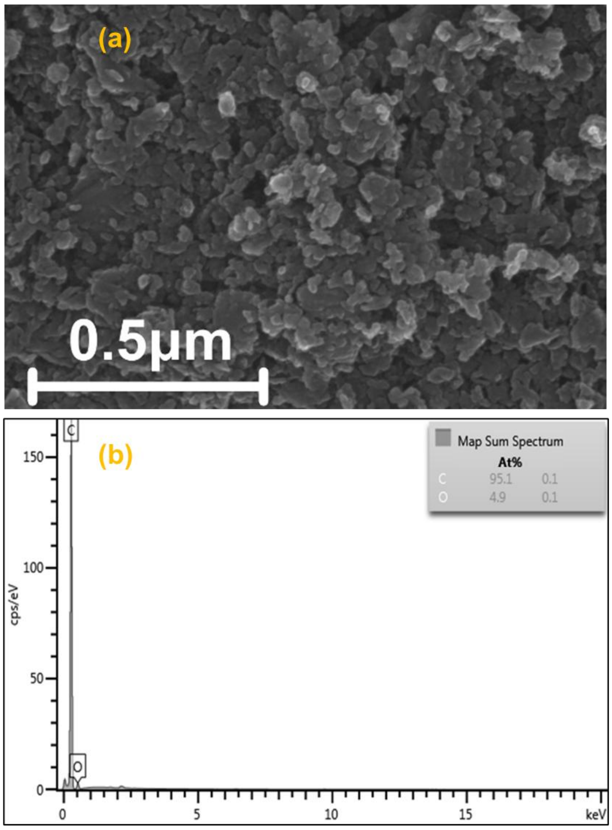

Fig. 2. (A) FE-SEM image and (B) Map sum spectrum of GNPs

structure could increase the multiple scattering of the material, thereby enhancing RAM performance. As illustrated in **Fig. 2B**, the EDS map sum spectrum of GNPs showed the presence of carbon and oxygen elements. The analysis revealed that the carbon content constituted 95.1% of the sample, while the oxygen content accounted for 4.9%. These results indicate that the GNPs are composed of pure carbon.

As illustrated in **Fig. 3a**, the TiO_2/GNP nanocomposites consisted of TiO_2 nanoparticles attached to the surface of layered GNPs. Furthermore, the analysis revealed that the TiO_2/GNP nanocomposites exhibited a more defective and amorphous surface. The bonding between TiO_2 and GNPs is a physical bond known as the mechanical interlocking model, as delineated in the formation mechanism. The attachment of the nanocomposites is evidenced by the distribution of elements seen in the

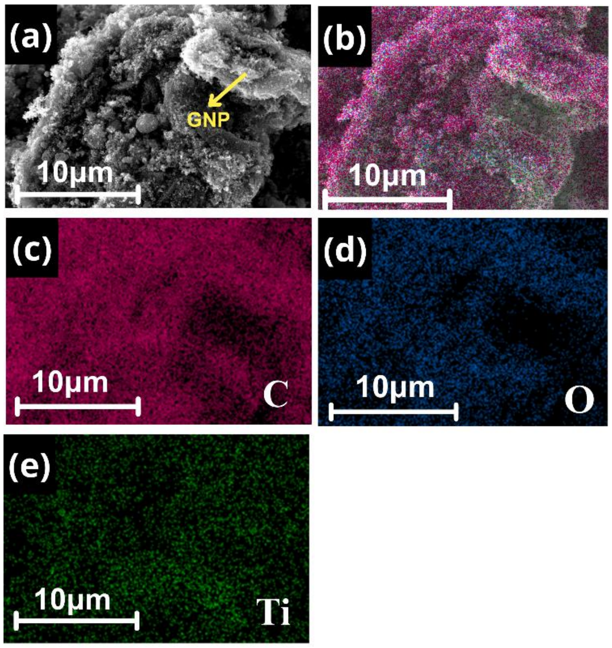

Fig. 3. FE-SEM images of a) TiO2/GNP nanocomposites and its EDS mapping results for of b) combined image c) C, d) O, and e) Ti

EDS mapping. As illustrated in **Fig. 3b**, the uniform distribution of elements suggests the successful formation of the nanocomposites. Moreover, the EDS mapping in **Fig. 3c, 3d,** and **3e** demonstrated the uniform distribution of C, O, and Ti elements across the material surfaces. The dispersion of the Ti element not only occurs on the surface of the material but also within the pores, thereby indicating that the formation process of nanocomposites has been achieved. **Fig. 4** presents a map sum spectrum of the TiO2/GNP nanocomposites,

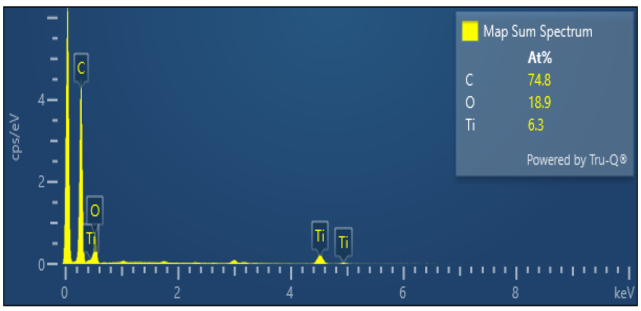

Fig. 4. Map sum spectrum of TiO_2/GNP nanocomposites

indicating a composition of 73.1% carbon, 19.7% oxygen, and 7.2% titanium elements.

Fig. 5 shows the X-ray diffractograms of GNPs, TiO_2, and the GNP/TiO_2 composites, which offer information about the crystal structure of each material. **Fig. 5a** shows the diffraction pattern of pure GNPs, as confirmed by JCPDS database No. 98-007-6767. It exhibited peaks at 2θ at 26.46° (002) and 44.43° (011). This diffraction pattern indicates that GNPs possess a crystal structure and properties similar to graphite. XRD analysis showed that GNPs had a hexagonal crystal system, the main characteristic of layered carbon.

Fig. 5b shows diffraction pattern of TiO_2 anatase that located at 25.30°, 37.79°, 48.03°, 53.89°, 55.06°, 62.68°, 68.76°, 75.04°, and 82.67°, which correspond to (011), (004), (020), (015), (121), (024), (116), (125), and (224) respectively as confirmed by JCPDS No. 98-017-2916. TiO_2 is comprised of three mineral phases: anatase, rutile, and brookite. The anatase phase is the most stable, in comparison to the other two TiO_2 phases [15]. The anatase phase of TiO_2 exhibits a tetragonal crystallite structure, accompanied by a band gap of 2.116 eV, which facilitates rapid electron distribution [16]. The band gap value can be determined using the UV-Vis test and subsequently calculating the tauc plot [17]. This attribute value of TiO_2 anatase contributes to its classification as a semiconductor.

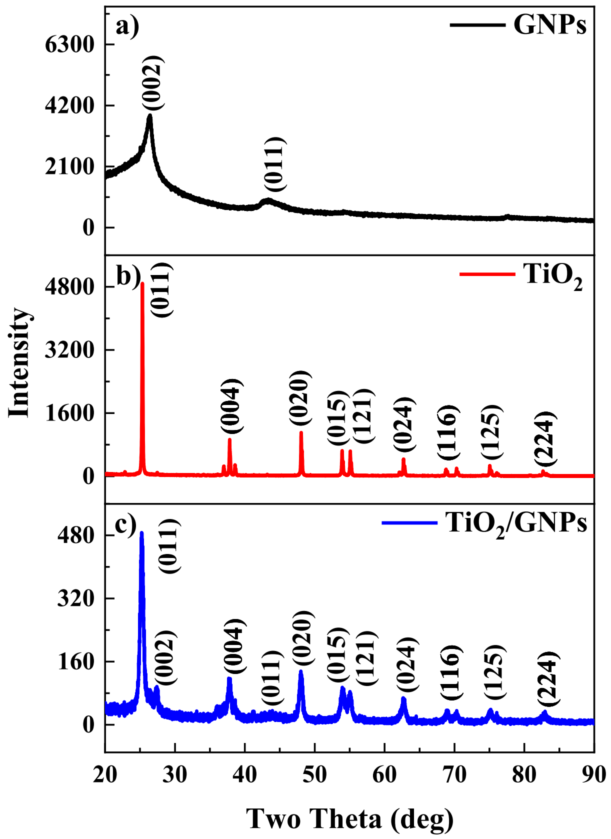

Fig. 5. XRD patterns of a) GNPs, b) TiO2, and c) TiO2/GNP nanocomposites

Figure 5c shows the XRD pattern of the TiO_2/GNP nanocomposites, revealing the presence of GNPs. The XRD pattern of the TiO_2/GNP nanocomposites showed the presence of minor peaks corresponding to GNPs (002) and (011). A comparison of the XRD patterns of pure TiO_2 and the TiO_2/GNP nanocomposites revealed that the nanocomposite had a more amorphous and impure pattern. The intensity of each peak decreased drastically. This decrease occurs due to the addition of carbon to the material. This finding suggests that TiO_2/GNP nanocomposites have been successfully formed.

From the results of the XRD analysis, the crystallite size of the material can be calculated using the Scherrer equation in Eq (1):

$$D = \frac{k\lambda}{\beta_{hkl}\cos\theta_{hkl}} \quad (1)$$

where: k is ineteger (0.9), λ is X-Ray wavelength (0.154 nm), β_{hkl} is full width at half maxim (FWHM) (Rad), and θ_{hkl} is Bragg-diffraction angle (peak positions in radian) (degree).

The FWHM, crystallinity percentage, and crystallite sizes calculated from the XRD analysis are summarised in **Table 1**. The addition of GNPs into the TiO_2 sample resulted in a decline in crystallinity, which could be attributed to the amorphous structure of GNPs. The crystallite size of GNPs synthesized by Latif et al. is 32.28 nm [18]. This value is smaller than that of the GNPs used in this study. In the research conducted by Saravanan et al., the crystallite size of the anatase TiO_2 utilized was measured to be 4.28 nm [19]. This value is also smaller than the TiO_2 utilized in this study. This discrepancy can be attributed to distinct types and brands of GNPs and TiO_2 used in the respective studies. Furthermore, the TiO_2/GNP nanocomposites exhibited smaller crystallite sizes than pure TiO_2. These outcomes indicate the effectiveness of the homogenization process of the TiO_2/GNP nanocomposites using the planetary ball milling method, leading to a reduction in material size.

Table 1. FWHM, crystallinity percentage, and crystallite size measurements from X-ray diffraction

Sample	FWHM (°)	Crystallinity (%)	Crystallite size (nm)
GNPs	0.336	-	24.37
TiO2	0.132	90.48	61.91
TiO2/GNs	0.48	72.64	16.99

3.3. Microwaves Absorbing Performance

The performance of microwave absorption was evaluated using a VNA. The VNA test is used to determine the reflection loss of the material to evaluate the performance of the RAM [20]. The reflection loss (RL) value indicates the ability of the material to absorb microwaves. The permittivity and permeability values influence the RL value. Permittivity ($\varepsilon = \varepsilon' - \varepsilon''$) is related to the dielectric value of the material. In comparison, permeability ($\mu = \mu' - \mu"$) is associated with the magnetic value of the material. The values of ε' dan μ' are related to the ability to store energy. While $\varepsilon"$ dan $\mu"$ are related to the energy lost due to heat [21]. The value of RL can be summarized in Eq (2) and (3):

$$Z_{in} = z_0\sqrt{\mu_r/\varepsilon_r}\tanh[j(2\pi fd)/c\sqrt{\mu_r/\varepsilon_r})] \qquad (2)$$

$$RL = 20\log\left|\frac{(Z_{in}-Z_o)}{(Z_{in}+Z_o)}\right| \qquad (3)$$

From the RL results, the value of the absorption coefficient or trough power can be found using Eq (4) and (5):

$$|\tau| = 10^{\text{reflection loss}/20} \qquad (4)$$

$$Through\ power\ (\%) = (1-\tau)\times 100\% \qquad (5)$$

Fig. 6. shows GNPs, TiO_2, and TiO_2/GNP nanocomposites. GNPs demonstrated a prominent absorption peak at a frequency of 8.31 GHz, accompanied by an RL of -30.44 dB and a through power of 99.90%. A thorough examination of the four primary absorptions within GNPs revealed that all of these absorptions had RLs below -10 dB, thereby ensuring a thorough power value higher than 90%. This condition proves that GNPs are a suitable material for use as a RAM. Moreover, GNPs have a layered structure that allows them to increase the interface polarization, and GNP properties permit them to conduct microwaves and convert them into heat, thereby increasing the RL value [22].

The VNA analysis of TiO_2 reveals unique characteristics absorption of TiO_2. The result analysis showed a maximum absorption frequency of 8.47 GHz, with an RL of -23.41 dB and a through power of 99.54%. Notably, three-absorption peaks in TiO_2 had RL below -10 dB and through power above 90%. These findings suggest that TiO_2 exhibits considerable dielectric

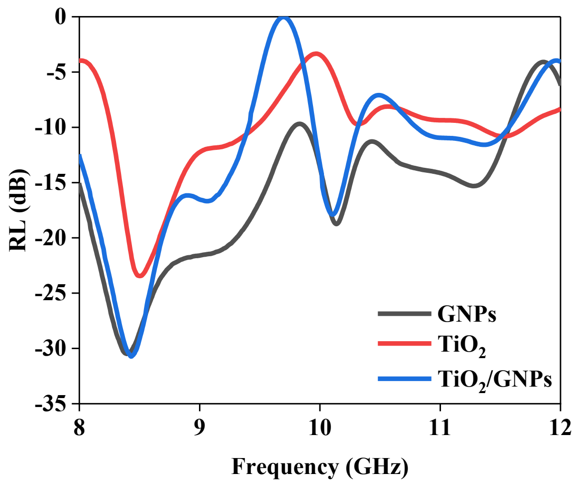

Fig. 7. VNA results of GNPs, TiO_2, and TiO_2/GNP nanocomposites

loss capacity, thereby enhancing the dipole interfaces and optimizing the reflection loss values [23].

TiO_2/GNP nanocomposites exhibited four primary absorption bands, with the most optimal absorption occurring at a frequency of 8.42 GHz, showing an RL of -30.72 dB and a through power of 99.91%. Notably, all RL values for TiO_2/GNP nanocomposites were below -10 dB and through power was above 90%. These findings indicate their suitability as RAM materials. Despite showing the lowest peak RL among all materials at a frequency of 8 GHz, as illustrated in **Table 2,** TiO_2/GNP nanocomposites showed reduced RL compared to pure GNPs. TiO_2 nanoparticles can introduce dielectric loss mechanisms, such as interfacial polarization and dipole relaxation. However, TiO_2 possesses a lower electrical conductivity than pure GNPs [24]. Therefore, the decrease in RL of the GNPs/TiO_2 composites is most likely due to the increased of polarization mechanisms and reduced conductivity loss resulting from the insulating properties of TiO_2.

Table 2. RL and through power of GNPs, TiO_2, and TiO_2/GNP nanocomposites

Sample	RL	Frequency	Through Power (%)
GNPs	-30.44	8.31	99.90
	-21.22	9.15	99.24
	-18.74	10.14	98.66
	-15.28	11.27	97.03
TiO_2	-23.41	8.47	99.54
	-11.64	9.22	93.14
	-9.76	10.32	89.43
	-10.78	11.51	91.64
TiO_2/GNPs	-30.72	8.42	99.91
	-16.67	9.08	97.84
	-17.87	10.11	98.36
	-11.57	11.37	93.03

CONCLUSION

TiO_2/GNP nanocomposites for radar-absorbing material successfully synthesized using the planetary ball milling method. FE-SEM observations showed that TiO_2 nanoparticles were attached to the surface of layered GNPs. Layered surface of GNPs could increase multiple scattering, thereby improving microwave absorption performance. XRD analysis showed a reduction in peak intensity for TiO_2/GNP nanocomposites compared to pure TiO_2 due to the addition of carbon elements. VNA analysis confirmed that TiO_2/GNP nanocomposites achieved optimum RL of -30.72 dB at a frequency of 8.42 GHz, with a through power of 99.91%. These findings indicated that TiO_2/GNP nanocomposites possess promising properties as the optimal radar-absorbing materials (RAMs).

SUPPORTING INFORMATION

There is no supporting information in this paper. The data supporting this research's findings are available on request from the corresponding author (RM).

ACKNOWLEDGEMENTS

We acknowledged the support from nanocarbon functional research group, National Innovation, and Research Agency, Tangerang Selatan.

CONFLICT OF INTEREST

There was no conflict of interest in this study

AUTHOR CONTRIBUTIONS

GRA, AH, ABR, IR, AS and RM were evenly contributed in this research. This study was designed and conducted by GRA, AH, and ABR, while IR and AS were the manager of the characterization. All authors were agreed to the final version of this manuscript.

REFERENCES

[1] Ivan Z.J.J. & Kim, Y. 2003. *Synthetic Aperture Radar*. In: Encyclopedia of Physical Science and Technology. Elsevier. pp 451–465.

[2] Qu, S., Wu, G., Fang, J., Zang, D., Xing, H., Wang, L., & Wu, H. 2017. *Dielectric and magnetic loss behavior of nanooxides*. In Spectroscopic Methods for Nanomaterials Characterization. 301-319. doi: 10.1016/B978-0-323-46140-5.00011-X.

[3] Nag, A., Simorangkir, R.B., Gawade, D.R., Nuthalapati, S., Buckley, J.L., O'Flynn, B., Altinsoy, M.E., & Mukhopadhyay, S.C. 2022. Graphene-based wearable temperature sensors: A review. *Mater. Des.* 221. 110971. doi: 10.1016/j.matdes.2022.110971.

[4] Wang, L., Aslani, F. 2019. A review on material design, performance, and practical application of electrically conductive cementitious composites. *Constr. Build Mater.* 229. 116892. doi: 10.1016/j.conbuildmat.2019.116892.

[5] Sathish, K.M., Joseph, A., James, R.K.C., Jayavel, R. 2025 Engineering multifunctionality graphene-based nanocomposites with epoxy-silane functionalized cardanol for next-generation microwave absorber. *J. Colloid Interface Sci.* 678. 407–420. doi: 10.1016/j.jcis.2024.08.193.

[6] Silva, A.A., Stein, R., Campos, D., Indrusiak, T., Soares, B.G., & Barra, G.M. 2019. Conducting materials based on epoxy/graphene nanoplatelet composites with microwave absorbing properties: effect of the processing conditions and ionic liquid. *Front. Mater.* 6. 156. doi: 10.3389/fmats.2019.00156.

[7] Qiao, J., Zhang, X., Xu, D., Kong, L., Lv, L., Yang, F., Wang, F., Liu, W., & Liu, J. 2020. Design and synthesis of TiO_2/Co/carbon nanofibers with tunable and efficient electromagnetic absorption. *Chem. Eng. J.* 380. 122591. doi: 10.1016/j.cej.2019.122591.

[8] Yang, Z., Luo, F., Hu, Y., Duan, S., Zhu, D., & Zhou, W. 2016. Dielectric and microwave absorption properties of TiO_2/Al_2O_3 coatings and improved microwave absorption by FSS incorporation. *J. Alloys Compd.* 678. 527-532. doi: 10.1016/j.jallcom.2016.04.031.

[9] Xia, T., Zhang, C., Oyler, N.A., & Chen, X. 2013. Hydrogenated TiO_2 nanocrystals: a novel microwave absorbing material. *Adv. Mater.* 25(47). 6905-6910. doi: 10.1002/adma.201303088.

[10] Zhang, H., Zhao, Y., Yang, X., Zhao, G., Zhang, D., Huang, H., Yang, S., Wen, N., Javid, M., Fan, Z. & Pan, L. 2020. A facile synthesis of novel amorphous TiO2 nanorods decorated rGO hybrid composites with wide band microwave absorption. *Nanomaterials.* 10(11). 2141. doi: 10.3390/nano10112141.

[11] Xu, J., Qi, X., Luo, C., Qiao, J., Xie, R., Sun, Y., Zhong, W., Fu, Q. & Pan, C. 2017. Synthesis and enhanced microwave absorption properties: a strongly hydrogenated TiO_2 nanomaterial. *Nanotechnology.* 28(42). 425701. doi: 10.1088/1361-6528/aa81ba.

[12] Mo, Z., Yang, R., Lu, D., Yang, L., Hu, Q., Li, H., Zhu, H., Tang, Z. & Gui, X. 2019. Lightweight, three-dimensional carbon Nanotube@ TiO_2 sponge with enhanced microwave absorption performance. *Carbon.* 144. 433-439. doi: 10.1016/j.carbon.2018.12.064.

[13] Park, S.J. & Seo, M.K., 2011. Solid-solid interfaces. *Interface science and technology.* 18. 253-331. doi: 10.1016/B978-0-12-375049-5.00004-9.

[14] Zheng, H., Zhang, W., Li, B., Zhu, J., Wang, C., Song, G., Wu, G., Yang, X., Huang, Y. & Ma, L. 2022. Recent advances of interphases in carbon fiber-reinforced polymer composites: A review. *Compos. B. Eng.* 233. 109639. doi: 10.1016/j.compositesb.2022.109639.

[15] Liu, X. and Fu, J. 2020. Electronic and elastic properties of the tetragonal anatase TiO_2 structure from first principle calculation. *Optik.* 206. 164342. doi: 10.1016/j.ijleo.2020.164342.

[16] Li, C., Dang, S., Zhang, C., Wang, L. & Han, P. 2014. Effects of native defects on the electronic structure and photocatalytic activity in anatase TiO_2 by first principles calculations. *Optik.* 125(13). 3145-3149. doi: 10.1016/j.ijleo.2013.12.010.

[17] Fleck, N., Amli, H., Dhanak, V. & Ahmed, W. 2021. Characterization techniques in energy generation and storage. In *Emerging Nanotechnologies for Renewable Energy.* 259-285. doi: 10.1016/B978-0-12-821346-9.00003-1.

[18] Latif, Z., Rehman, A.U., Amin, N., Arshad, M.I. & Marzouki, R. 2023. Graphene nanoplatelets (GNPs): a source to bring change in the properties of Co–Ni–Gd-ferrite/GNP nanocomposites. *RSC Adv.* 13(49). 34308-34321. doi: 10.1039/D3RA02080K.

[19] Saravanan, S. & Dubey, R.S. 2021. Optical and morphological studies of TiO_2 nanoparticles prepared by sol–gel method. *Mater. Today Proc.* 47. 1811-1814. doi: 10.1016/j.matpr.2021.03.207.

[20] Zhang, H., Krooswyk, S. & Ou, J. 2015. High speed digital design: design of high speed interconnects and signaling. Elsevier. 199–219.

[21] Elmahaishi, M.F., Azis, R.A.S., Ismail, I. & Muhammad, F.D., 2022. A review on electromagnetic microwave absorption properties: their materials and performance. *J. Mater. Res. Technol.* 20. 2188-2220. doi: 10.1016/j.jmrt.2022.07.140.

[22] Wang, G., Li, C., Estevez, D., Xu, P., Peng, M., Wei, H. & Qin, F. 2023. Boosting interfacial polarization through heterointerface engineering in MXene/graphene intercalated-based microspheres for electromagnetic wave absorption. *Nanomicro. Lett.* 15(1). 152. doi: 10.1007/s40820-023-01123-4.

[23] Li, C., Deng, L., He, J., Peng, S., Huang, S. & Qiu, L. 2023. Multi-interfacial TiO_2/carbon fibers encapsulated with needle-like $FeCo_2O_4$ for excellent microwave absorption. *Appl. Surf. Sci.* 629. 157417. doi: 10.1016/j.apsusc.2023.157417.

[24] Tao, E., Ma, Z., Yang, S., Li, Y., Ma, D., Xing, Z. & Li, Y. 2020. Enhanced electrical conductivity of TiO_2/graphene: The role of introducing Ca^{2+}. *J. Alloys Compd.* 827. 154280. doi: 10.1016/j.jallcom.2020.154280.